ELSEVIER

International Journal of Mass Spectrometry 184 (1999) 89–101

International Journal of Mass Spectrometry

Carbonylation of ammonia by gaseous FCO^+. A *G*2 and Rice-Ramsperger-Kassel-Marcus study of the detailed mechanistic aspects

Massimiliano Aschi, Felice Grandinetti*

Dipartimento di Scienze Ambientali, Università della Tuscia, Via S. C. De Lellis, 01100 Viterbo, Italy

Received 12 October 1998; accepted 28 November 1998

Abstract

The detailed mechanism of the gas-phase carbonylation of NH_3 by FCO^+ with formation of H_2NCO^+ and HF has been theoretically investigated by *G*2 and Rice-Ramsperger-Kassel-Marcus (RRKM) calculations. The results provide a coherent description of the experimental evidence, so far obtained by Fourier transform ion cyclotron resonance spectrometry. The detailed *G*2 potential energy surface of the reaction has been used to outline the corresponding kinetic scheme, whose rigorous formulation has been simplified by making assumptions based on the explicit evaluation of all the involved kinetic constants, calculated according to the RRKM theory. It was possible to estimate the efficiency of the reaction for different alternative mechanisms and to compare the obtained values with the experimentally measured efficiency, used as a probing reference value. The obtained results indicate that the reaction occurs by a "composite" mechanism, which involves the initial formation of an adduct between FCO^+ and NH_3 and the subsequent loss of HF by two distinct paths. In addition, it was possible to conclude that the only ionic product expected from the reaction is the $H_2N–CO^+$ isomer. (Int J Mass Spectrom 184 (1999) 89–101) © 1999 Elsevier Science B.V.

Keywords: Gaseous FCO^+; G2 theory; RRKM theory; Carbonylation reaction

1. Introduction

The fluorocarbonyl cation FCO^+ is a prototype species of considerable interest [1]. The theoretical studies reported to date [2–9] invariably predict that this ion resides in a deep potential well. However, its successful observation strongly depends on the choice of the experimental conditions. In the condensed phase, the preparation of FCO^+ is challenging [10], and it is therefore not surprising that the recent observation by Olah, Prakash, and co-workers of FCO^+ under superacid stable ion conditions [11] has been emphasized [1] as a new development in superacid chemistry. In the gaseous phase, FCO^+ is instead quite stable and easily produced from the electron-impact ionization of several neutrals, e.g. HFCO [12a], F_2CO [12b,13], ClFCO [12b], and CH_3COF. Therefore, if one works under the isolated conditions typical of the mass spectrometric experiments, it is possible to investigate the intrinsic aspects of the chemistry of FCO^+. In particular, Grandinetti et al. have recently reported an extensive study [14] on the formation of gaseous FCO^+ by chemical routes

* Corresponding author.

PII S1387-3806(98)14278-1

and its reactivity toward exemplary inorganic and organic neutrals. The observation of the following efficient reactions

$$FCO^+ + NH_3 \rightarrow H_2NCO^+ + HF \quad (1)$$

$$FCO^+ + C_6H_5\text{–}X \rightarrow X\text{–}C_6H_4\text{–}CO^+ + HF \ (X = H, CH_3, F, Cl) \quad (2)$$

was of particular interest as they are novel examples of gas-phase electrophilic carbonylations and simple models for the coupled activation of CO and inert N–H and C–H bonds. With the aim of learning more on the practically unexplored mechanistic aspects of the chemistry of FCO^+ and attracted by the small size of the ions and neutrals involved in reaction (1), we decided to undertake a detailed computational study of this process. The results of the joint application of the *G*2 [15] and Rice-Ramsperger-Kassel-Marcus (RRKM) [16] theories provide a description of the elementary steps conceivably involved in this formally simple addition-elimination reaction which is fully coherent with the available experimental data.

2. Computational details

The ab initio calculations have been performed using the GAUSSIAN 94 [17] and GAMESS [18] sets of programs. The geometries of the investigated species were optimized, within the specified symmetry constraints, at the HF/6-31*G*(*d*) and MP2/6-31*G*(*d*) level of theory [the latter was used with no frozen core orbitals and will be denoted as MP2(FULL)/6-31*G*(*d*)] and their harmonic vibrational frequencies were computed at both computational levels. Approximate QCISD(T)/6-311+*G*(3*df*,2*p*) total energies were calculated at the MP2(FULL)/6-31*G*(*d*) optimized geometries using the *G*2 procedure [15]. This computational method is amply recognized [19] as able to reproduce or predict unknown thermochemical data (atomization energies, ionization potentials, electron affinities, and proton affinities) of compounds containing first- and second-row atoms with a target accuracy of $\pm$ 2 kcal mol^{-1}. Whereas the 6-31*G*(*d*) basis set includes six *d*-type functions, all the other basis sets employ five *d*-type and, if included, seven *f*-type functions. In addition, all the single-point calculations treat electron correlation only for the valence electrons (the frozen-core approximation). Within the *G*2 theory, *E*(ZPE) is derived from the HF/6-31*G*(*d*) frequencies scaled by 0.8929, and the obtained total energy refers to 0 K. This *G*2(0 K) has been corrected to 298.15 K, *G*2(298.15 K), by adding the translational (3/2 RT), rotational (RT or 3/2 RT for linear and nonlinear species, respectively), and vibrational contributions at this temperature. The last term has been calculated by standard statistical mechanics formulas [20] using the scaled HF/6-31*G*(*d*) vibrational frequencies.

The kinetic constants k_i of the single unimolecular elementary steps involved in the overall reaction (1) have been evaluated using the RRKM theory [16]. In the employed formula

$$k_i(E) = N^*(E - E_0)/[h\rho(E)]$$

E is the total energy of the reactant ion, E_0 is the activation energy, i.e. the minimum energy value for which the rate constant has its minimum nonzero value, $N^*(E - E_0)$ is the sum of the rotovibrational states of the transition structure at energy $(E - E_0)$, and $\rho(E)$ is the density of the states of the reactant ion at energy E, i.e. the number of quantum states per unit energy. The values of $\rho(E)$ and $N^*(E - E_0)$ for the calculation of the kinetic constants of the unimolecular reactions involving a "tight" transition structure have been calculated by the Beyer and Swinehart algorithm [21] using the MP2(FULL)/6-31*G*(*d*) harmonic frequencies and moments of inertia of the involved minimum and transition structure, respectively. The values of $N^*(E - E_0)$ for the calculation of the kinetic constants of the unimolecular dissociation reactions which occur with no energy barrier have been obtained using the variational transition state theory [22]. Accordingly, the "loose" transition structure, R^*, lies in the region of the Born-Oppenheimer surface in correspondence of which the sum of the rotovibrational states is minimum, i.e. $(dN^*/dR)_{R^*} = 0$. To find this condition, we have located,

along the reaction coordinate of the dissociation reaction, 10 different points by fixing the bond distance between the two dissociating moieties and optimizing all the remaining internal coordinates (the MP2(FULL)/6-31$G(d)$ level of theory appears not inadequate because the presently investigated complexes heterolytically dissociate into an ion and a neutral whose recombination energy and ionization potential, respectively, differ by at least 1 eV). The hessian matrices **H** calculated at these nonstationary points do not have any physical meaning and have been converted to **H′** according to the expression [23]

$$\mathbf{H}' = (\mathbf{1} - \mathbf{P})\mathbf{H}(\mathbf{1} - \mathbf{P})$$

The matrix **P** is chosen so to project out of **H** the mode corresponding to the reaction coordinate as well as the infinitesimal rotational and translational modes. For each of the 10 included points, the diagonalization of **H′** provides the $3N - 7$ eigenvalues and the vibrational frequencies used, together with the moments of inertia, to calculate the sum of the states.

3. Results and discussion

3.1. The reaction of FCO^+ with NH_3: previous experimental findings

The occurrence of reaction (1) has been so far ascertained [14] using Fourier transform ion cyclotron resonance (FTICR) spectrometry [24]. The FCO^+ ions prepared in the external source of the instrument by electron impact ionization of CH_3COF or NF_3/CO mixtures were transferred into the resonance cell, isolated, thermalized by unreactive collisions with pulsed-in argon, and allowed to react with NH_3. Their intensity was found to decrease exponentially over the entire time interval and the elemental composition of the only observed primary ionic product was unambiguously assigned as H_2NCO^+ by exact mass measurements. The rate constant of reaction (1) was measured as 1.0×10^{-9} cm^3 mol^{-1} s^{-1}, with an estimated error of $\sim\pm$ 30%. Therefore, the overall efficiency of the process is obtained as 0.60 ± 0.20 from the ratio of the experimental rate constant and the collision rate constant, evaluated as 1.69×10^{-9} cm^3 mol^{-1} s^{-1} from the average dipole orientation (ADO) theory [25].

3.2. The reaction of FCO^+ with NH_3: outline of the G2 potential energy surface

The potential energy surface conceivably involved in reaction (1) has been outlined by locating the various minima and transition structures at the MP2(FULL)/6-31$G(d)$ level of theory and refining their total energies up to the $G2$ level of theory. The geometries of all the obtained species are shown in Figs. 1 and 2, respectively, and their total and relative energies are collected in Table 1.

Our observed reaction (1) conceivably commences by formation of a complex between FCO^+ and NH_3. Consistent with the theoretical description of FCO^+ as a C electrophile [10], we have located the tightly bound adducts of C_s symmetry **1a** and **1b**. However, only **1a** revealed to be a true minimum on the surface, whereas **1b** was characterized as a first order saddle point, unstable with respect to the rotation of the hydrogen atoms around the C–N bond. This motion is predicted as practically barrier free from the vanishingly small energy difference of the two ions. The relatively short C–N distance of **1a**, 1.520 Å, and the significant deformation of the F–C–O moiety with respect to the linearity of the FCO^+ ion suggest an appreciable interaction between FCO^+ and NH_3. In fact, from Table 1, the association energy of these two fragments with formation of **1a** results as large as 70.9 kcal mol^{-1}.

If one assumes the initial formation of **1a**, the simplest reaction path to the experimentally observed products of reaction (1) is the “direct” HF elimination, with formation of ions of H_2N–CO^+ connectivity. We have ascertained that this process involves the isomerization of **1a** into isomer **3**, a loosely bound adduct between H_2N–CO^+ and HF whose dissociation into these two fragments requires only 11.4 kcal mol^{-1}. The isomerization of **1a** into **3** passes through the transition structure of C_s symmetry **TSNF**, and requires to overcome an activation barrier of 47.9 kcal mol^{-1}.

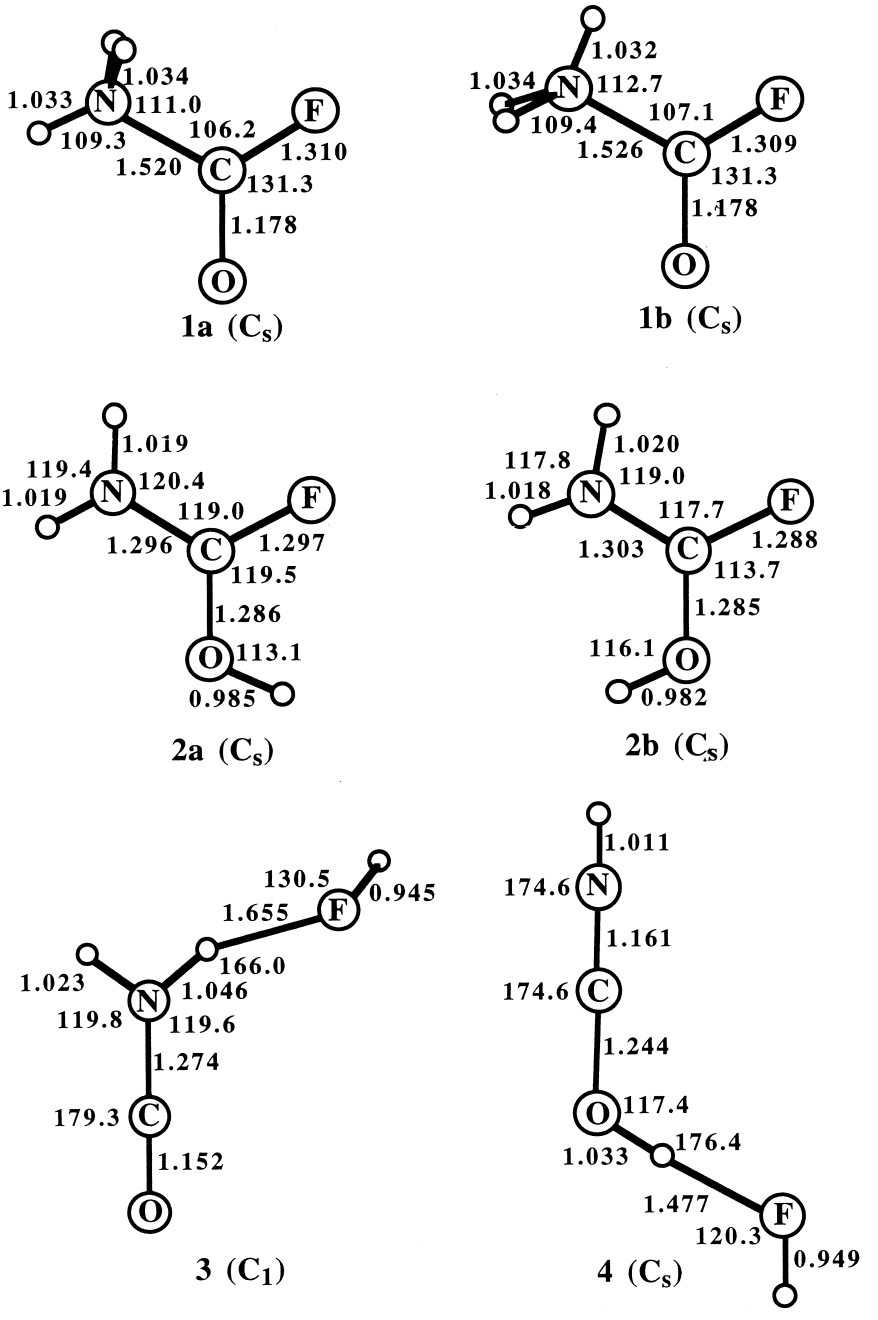

Fig. 1. MP2(FULL)/6-31$G(d)$ optimized parameters of the $(FCONH_3)^+$ isomers **1–4**. Bond lengths are in Ångstroms, bond angles in degrees, and the unlabelled circles are hydrogen atoms.

An alternative mechanistic path to the products observed from reaction (1) involves the isomerization of the initially formed isomer **1a** to the carbonium ions of connectivities **2a** and **2b**. Both of these structures have been located as true minima of C_s symmetry, and **2a** was found to be more stable than

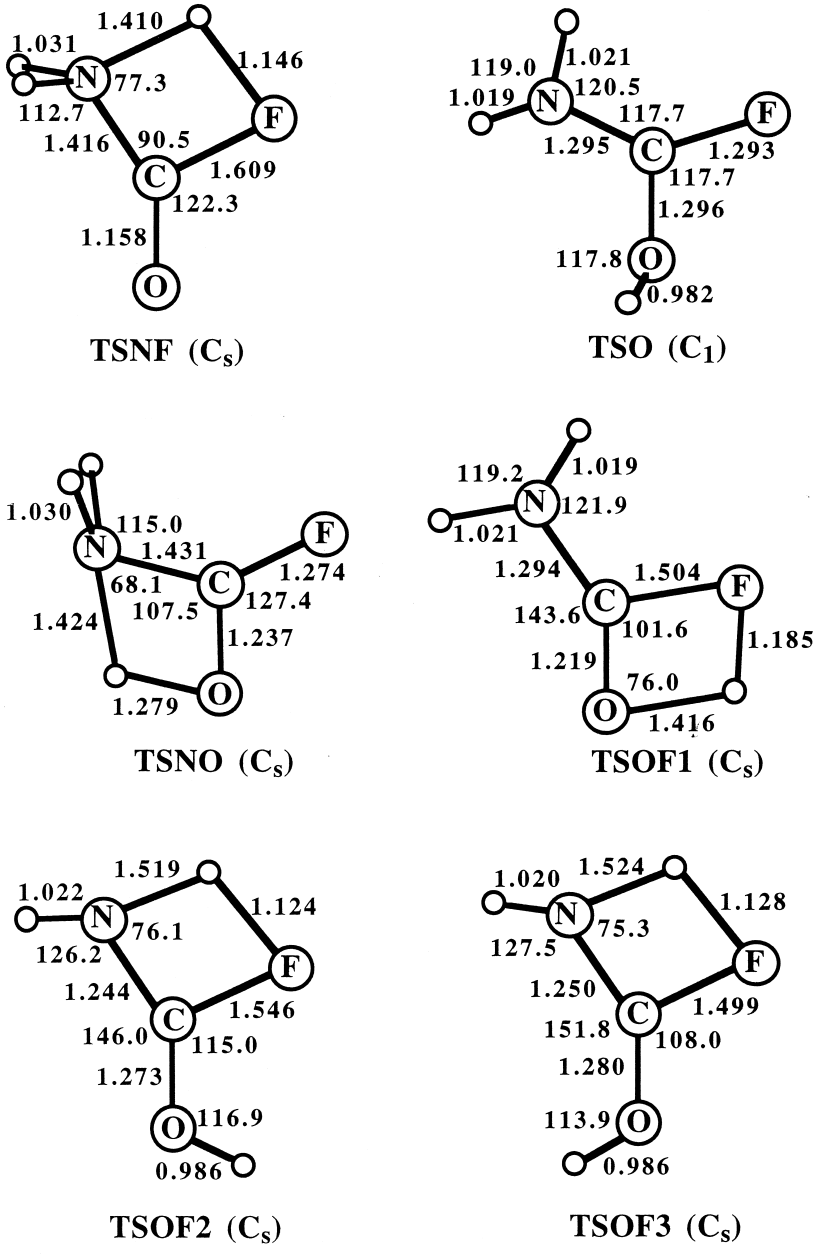

Fig. 2. MP2(FULL)/6-31$G(d)$ optimized parameters of the $(FCONH_3)^+$ transitions structures. Bond lengths are in Ångstroms, bond angles in degrees, and the unlabelled circles are hydrogen atoms.

2b by 4 kcal mol^{-1}. From Fig. 1, this order of stability is likely because of the unfavourable eclipsing of two hydrogen atoms in ion **2b**, which reflects, for example, in the difference between the N–C–O angle of **2a**, 121.5°, with respect to **2b**, 128.6°. Isomer **2b** can be formed directly from **1a** passing through the transition structure of C_s symmetry **TSNO**, which requires an energy barrier of 41.9 kcal mol^{-1}. The formation of

Table 1
Zero-point energies and total energies (atomic units) and relative energies (kcal mol^{-1}) of the $(FCONH_3)^+$ ions and their fragments

Species (NIMAG[a])	ZPE[b]	*G*2 (0 K)	*G*2 (298.15 K)	ΔE (298.15 K)
1a (0)	0.050 78	−269.093 49	−269.089 17	0.0
1b (1)	0.050 53	−269.092 72	−269.089 11	+0.04
2a (0)	0.049 99	−269.114 98	−269.111 00	−13.7
2b (0)	0.049 93	−269.108 64	−269.104 65	−9.7
3 (0)	0.043 43	−269.098 90	−269.092 39	−2.0
4 (0)	0.042 44	−269.077 41	−269.071 25	+11.2
TSNF (1)	0.043 69	−269.017 03	−269.012 85	+47.9
TSO (1)	0.048 60	−269.099 72	−269.096 01	−4.3
TSNO (1)	0.045 07	−269.026 30	−269.022 44	+41.9
TSOF1 (1)	0.043 48	−269.022 70	−269.018 72	+44.2
TSOF2 (1)	0.042 16	−268.996 58	−268.992 29	+60.8
TSOF3 (1)	0.042 90	−268.995 43	−268.991 42	+61.3
FCO^+ (0)	0.010 93	−212.523 11	−212.520 38	
				+70.9
NH_3 (0)	0.033 04	−56.458 65	−56.455 78	
$H_2N–CO^+$ (0)	0.032 67	−168.730 08	−168.726 55	
				+9.4
HF (0)	0.008 86	−100.350 01	−100.347 65	
HN–C–OH^+ (0)	0.031 37	−168.703 86	−168.700 18	

[a] Number of imaginary frequencies.
[b] Scaled HF/6-31*G*(*d*).

2a from **2b** occurs through the transition structure of C_1 symmetry **TSO** and requires 5.4 kcal mol^{-1}. As expected, it occurs by the out-of-plane rotation of the OH moiety.

The elimination of HF from isomer **2a** can in principle occur by two distinct paths, with formation of two distinct isomeric H_2NCO^+ ions. Thus, from Fig. 1, whereas the HF elimination, which involves the OH moiety, leads to the formation of ions of $H_2N–CO^+$ connectivity, the HF elimination, which involves the NH_2 moiety, leads to the formation of the alternative HN–C–OH^+ isomer. Thermochemical considerations [26] suggest that the latter process is as well conceivable. In fact, assuming the formation of the $H_2N–CO^+$ isomer and using the enthalpy of formation of the FCO^+ ion of 178.1 ± 2.3 kcal mol^{-1} recently determined by photoionization mass spectrometry [27], reaction (1) results exothermic by 65.2 kcal mol^{-1}. From Table 1, within the combined uncertainties of the experimental and theoretical values, this is consistent with the *G*2(298.15 K) estimate of 61.5 kcal mol^{-1} and provides reassuring evidence on the adequacy of the *G*2 theory in correctly predicting the relative stability of the presently investigated $(FCONH_3)^+$ ions. The experimental enthalpy of formation of the HN–C–OH^+ isomer is not available. Therefore, the evaluation of the enthalpy change of reaction (1) assuming the formation of this ion can only rest on theoretical estimates. From Table 1, we obtain a *G*2(298.15 K) value of −45.0 kcal mol^{-1}. Thus, irrespective of the assumed $H_2N–CO^+$ and HN–C–OH^+ ionic product, reaction (1) is predicted to be largely exothermic, which is consistent with its actual observation as an efficient process under FTICR conditions. We note that our computed *G*2(298.15 K) energy difference of 16.5 kcal mol^{-1} between the $H_2N–CO^+$ and HN–C–OH^+ isomers is in line with previous theoretical estimates of the relative stability of the isomeric ions from the gas-phase protonation of HN–CO [28].

The HF elimination from isomer **2a** with formation of ions of $H_2N–CO^+$ connectivity occurs by isomerization into isomer **3** and subsequent dissociation of this adduct. This process passes through the transition structure of C_s symmetry **TSOF1** and requires 57.9 kcal mol^{-1}. The HF elimination from **2a** with forma-

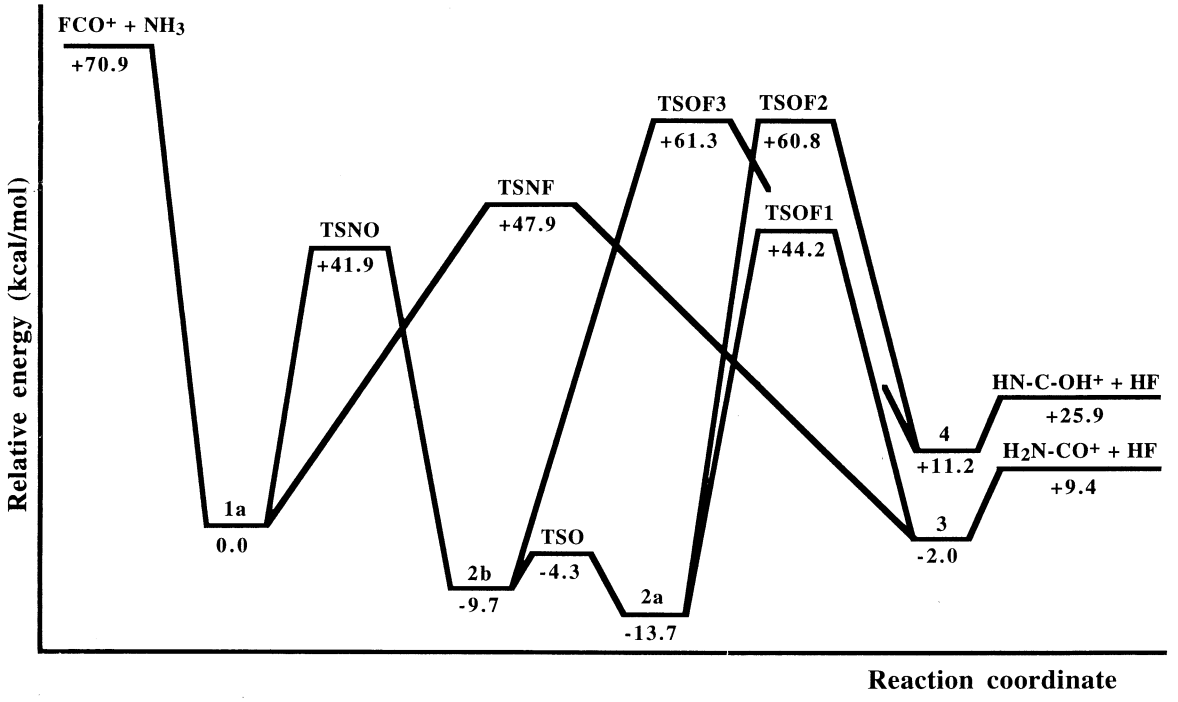

Fig. 3. *G2*(298.15 K) relative energies of the $(FCONH_3)^+$ ions and their fragments.

tion of the HN–C–OH^+ isomer involves the isomerization into the C_s-symmetry isomer **4**, a loosely bound adduct between HN–C–OH^+ and HF whose dissociation into these two fragments requires 14.7 kcal mol^{-1}. The isomerization of **2a** into **4** passes through the transition structure of C_s symmetry **TSOF2** and requires to overcome an energy barrier of 74.5 kcal mol^{-1}. Finally, we have investigated the conceivable occurrence of the formation of the HN–C–OH^+ isomer by HF elimination from isomer **2b**. This process involves the isomerization of **2b** into **4** and occurs through the transition structure **TSOF3**. It demands an activation energy of 71.0 kcal mol^{-1}. From Fig. 2, **TSOF2** and **TSOF3** are indeed structurally similar and it is therefore not surprising that, at the *G*2(298.15 K) level of theory, they are practically degenerate.

The *G*2 relative energies at 298.15 K of all the above minima and transition structures are diagramatically shown in Fig. 3.

3.3. The reaction of FCO^+ with NH_3: outline of the kinetic scheme

Following the characterization of the potential energy surface conceivably involved in reaction (1), we have focused attention on its kinetic aspects. The full sequence of the isomerization and dissociation reactions schematized in Fig. 3 is shown in Chart 1. This rigorous formulation of the kinetic scheme of reaction (1) does not make easily treatable the derivation of steady-state equations which relate the overall efficiency of reaction (1) with the kinetic constants of its single elementary steps (vide infra). It is however possible to make simplifying assumptions which are based on the explicit evaluation of the kinetic constants $k_i s$ which appear in Chart 1. Apart from k_1, assumed to be equal to the ADO value, all the other $k_i s$ have been calculated using the microcanonical transition state theory in the RRKM formulation [16]. This approach, usually employed to de-

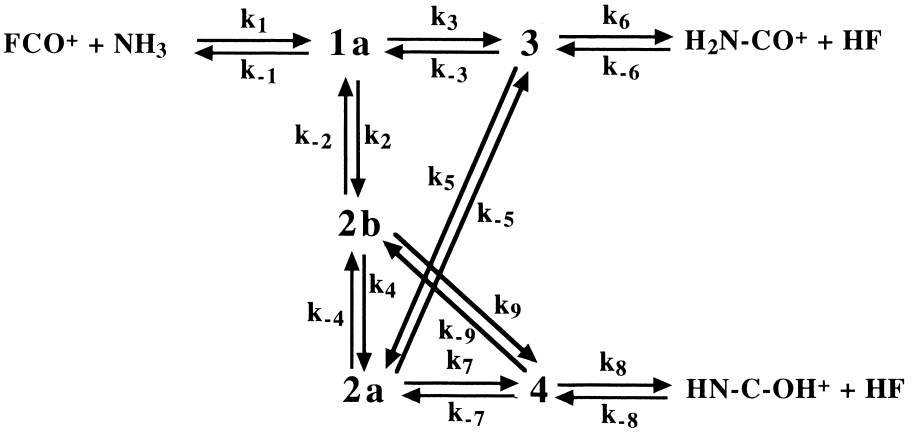

Chart 1.

scribe reactions that occur under the isolated and nonthermal conditions of the FTICR experiment, appears in particular adequate for the presently investigated reaction (1). In fact, if the basic ergodic assumption [22] would not be actually verified along the overall reaction path, owing to the appreciable height of all the calculated *G*2 energy barriers, a slow randomisation of the internal energy starting from the initially populated mode corresponding to the path leading to the formation of **1a** could hardly result in an overall efficiency experimentally measured as high as 0.6 ± 0.2. We feel it is also appropriate to comment here on the fact that the values of the imaginary frequencies of the transition structures involved in the various hydrogen migrations, computed in the range of $\sim 1500i$–$1800i$ cm^{-1}, could suggest an appreciable influence of tunneling [29] on the kinetic constants. However, we decided not to include this effect in our calculations by noting that, based on our computed *G*2 potential energy profile, under the isolated conditions of the FTICR experiments, the energies of all the intermediates involved in the various elementary steps of reaction (1) could hardly result lower than the corresponding transition structures.

The details of the procedure employed to calculate $k_i s$ have been given earlier and we present here only the relevant results.

According to the RRKM theory, the kinetic constants of all the unimolecular reactions reported in Chart 1 critically depend on the internal energy content of the reacting ion. From Fig. 3, the latter value is determined from the internal energy **E** of the encounter complex **1a** and the energy difference between **1a** and the reacting ion. Assuming **E** as the energy content of 73.6 kcal mol^{-1} of **1a** with respect to the FCO^+ and NH_3 reagents at 298.15 K appears quite plausible. In fact, our observed reaction (1) involves FCO^+ ions that are thermalized by unreactive collisions with argon and react at room temperature with NH_3 at a stationary pressure at 298.15 K. Still, we have calculated the kinetic constants $k_i s$ for different values of **E** ranging from 70.1–85.0 kcal mol^{-1} and assuming the rotational momentum distribution as that of a microcanonical ensemble. The lower limit corresponds to the energy difference at 0 K between the reagents and the encounter complex **1a**, whereas the upper limit is the energy at which the calculated efficiency of reaction (1) becomes negligible irrespective of the assumed reaction mechanism (vide infra). The kinetic constants $k_i s$ calculated for different values of **E** using the vibrational frequencies and moments of inertia reported in Tables 2 and 3 are collected in Table 4.

We note here that we refrained from the considerably time-consuming procedure required to calculate the kinetic constant k_8 of the dissociation of **4** into $HN–C–OH^+$ and HF according to the "loose" transi-

Table 2
MP2(FULL)/6-31$G(d)$ vibrational frequencies (cm^{-1}) and moments of inertia (atomic units) of the $(FCONH_3)^+$ isomers **1–4**

1a	1b	2a	2b	3	4
		Vibrational frequencies			
137.9	109.4*i*	484.4	464.1	46.6	89.8
426.8	433.3	495.4	510.4	84.1	115.8
577.0	576.5	551.0	584.1	262.7	304.4
596.9	604.0	680.0	651.3	300.5	305.5
814.0	809.4	699.7	674.4	388.7	447.5
1050.7	1029.0	745.9	752.0	515.4	509.1
1102.5	1103.1	1029.0	1048.0	564.0	544.3
1247.5	1250.4	1111.1	1097.5	741.8	611.8
1548.9	1547.4	1210.8	1170.1	1185.9	698.9
1681.8	1682.0	1606.8	1629.7	1233.2	1243.6
1684.0	1683.4	1644.6	1677.3	1636.3	1343.0
2018.1	2018.4	1860.2	1811.1	2390.9	2481.7
3359.6	3365.0	3546.2	3546.9	3157.0	2784.0
3461.2	3465.1	3637.3	3663.2	3562.5	3763.1
3479.8	3484.6	3666.8	3673.2	3917.7	3864.6
		Moments of inertia			
170.3	170.4	164.3	162.3	90.9	65.6
185.3	186.4	169.5	171.1	649.9	638.3
345.6	346.8	333.8	333.4	740.1	703.9

tion state theory. We assumed it to be of the same order of magnitude as the kinetic constant k_6 of the dissociation of **3** into $H_2N–CO^+$ and HF. This appears plausible, because, from Table 1, the energy changes of these two processes are quite similar.

The obtained values of the kinetic constants support the following simplifying assumptions to the kinetic scheme reported in Chart 1. First, we neglect the kinetic constants k_{-3} and k_{-5} of the back-isomerization of isomer **3** into **1a** and **2a**, respectively, with respect to the exceedingly larger constant k_6. Similarly, the kinetic constants k_{-7} and k_{-9} of the back isomerization of isomer **4** into **2a** and **2b**, respectively, can be safely neglected with respect to the exceedingly larger constant k_8. In addition, because the eventual formation of the products from reaction (1) under our FTICR conditions is indeed irreversible, both the kinetic constants k_{-6} and k_{-8} are set to zero. Second, the values of the kinetic constants k_4 and k_{-4} result exceedingly large, and it is therefore possible to regard the rotational motion which allows the interconversion of the conformers **2a** and **2b** as a free rotor. Third, we note that, irrespective of the assumed value of **E**, the kinetic constant k_5 of the isomerization of **2a** into **3** is significantly larger than the kinetic constant k_7 of the isomerization of **2a** into **4** and the kinetic constant k_9 of the isomerization of **2b** into **4**. Therefore, both k_7 and k_9 could be safely neglected with respect to k_5. However, in order to quantitatively appreciate the small contribution of the reaction paths involving the high-energy transition structures **TSOF2** and **TSOF3**, we decided to neglect only the smallest k_9. It means that we are assuming that the in case HF elimination from the rapidly interconverting isomers **2a** and **2b** with formation of the $HN–C–OH^+$ isomer occurs exclusively through the transition structure **TSOF2**.

According to these assumptions, we take as the actual kinetic scheme of reaction (1) the sequence of isomerization and dissociation processes depicted in Chart 2.

3.4. The mechanism of the reaction of FCO^+ and NH_3

The $G2$ relative energies reported in Fig. 3 are expected to be as accurate as ~2 kcal mol^{-1}. Still,

Table 3
MP2(FULL)/6-31$G(d)$ vibrational frequencies (cm^{-1}) and moments of inertia (atomic units) of the $(FCONH_3)^+$ transition structures

TSNF	TSO	TSNO	TSOF1	TSOF2	TSOF3
		Vibrational frequencies			
1471.3i	584.6i	1855.8i	1789.0i	1471.0i	1457.8i
156.2	501.7	313.3	426.4	73.2	364.9
441.0	576.6	498.8	479.0	439.1	483.7
513.0	675.2	586.2	591.8	577.5	589.9
625.1	730.5	741.0	605.5	623.4	665.6
847.7	769.3	1003.7	680.7	724.9	723.6
1003.0	1032.7	1062.4	826.7	809.9	846.1
1154.2	1063.7	1208.4	942.7	910.7	918.2
1196.4	1124.1	1301.6	1138.7	1045.0	1028.4
1258.6	1582.7	1434.0	1335.5	1169.8	1136.9
1633.9	1626.0	1645.5	1639.1	1243.0	1345.0
2010.6	1818.2	1789.2	2015.1	2040.4	1982.8
2203.5	3531.4	2069.1	2095.7	2139.9	2160.9
3424.6	3652.0	3432.5	3530.0	3585.1	3600.4
3511.8	3674.6	3522.7	3649.0	3624.5	3629.0
		Moments of inertia			
162.2	165.0	145.6	146.2	153.9	151.0
267.9	172.5	198.6	199.1	198.2	193.8
359.9	332.8	334.0	345.3	352.1	344.8

they do not furnish a safe indication on the detailed mechanism of reaction (1). In fact, whereas we could suggest that the routes involving the high-energy transition structures **TSOF2** and **TSOF3** should play a minor role, if any, it is difficult to appreciate by qualitative arguments the alternative or competitive occurrence of the reaction paths which involve the comparably stable transition structures **TSNO**, **TSNF**, and **TSOF1**. It is however possible to get more detailed information on the mechanism of reaction (1) using kinetic arguments. In particular, we note that the overall efficiency of reaction (1), **Eff(1)**, depends solely on the kinetic constants of its single elementary steps. Therefore, if one assumes that reaction (1)

Table 4
Kinetic constants of the elementary steps reported in Chart 1 as a function of the energy content **E** of the intermediate **1a**

E (kcal mol^{-1})							
k_i	70.1	72.1	73.6	75.5	77.0	80.0	85.0
k_{-1}	0.0	8.0E + 8	2.0E + 9	8.0E + 9	2.0E + 10	1.4E + 11	1.8E + 11
k_2	1.1E + 9	1.5E + 9	1.9E + 9	2.5E + 9	3.0E + 9	4.2E + 9	7.1E + 9
k_{-2}	5.6E + 8	7.8E + 8	9.7E + 8	1.2E + 9	1.6E + 9	2.3E + 9	4.1E + 9
k_3	6.5E + 8	9.8E + 8	1.3E + 9	1.8E + 9	2.3E + 9	3.7E + 9	7.3E + 9
k_{-3}	3.0E + 5	4.7E + 5	6.2E + 5	8.6E + 5	1.1E + 6	1.7E + 6	3.4E + 6
k_4	5.0E + 12	5.8E + 12	5.8E + 12	5.9E + 12	6.0E + 12	6.2E + 12	6.4E + 12
k_{-4}	3.3E + 12	3.4E + 12	3.5E + 12	3.6E + 12	3.7E + 12	3.8E + 12	4.0E + 12
k_5	7.8E + 8	1.1E + 9	1.4E + 9	1.8E + 9	2.2E + 9	3.3E + 9	6.1E + 9
k_{-5}	1.3E + 6	1.7E + 6	2.1E + 6	2.7E + 6	3.2E + 6	4.6E + 6	7.7E + 6
k_6	4.8E + 11	4.9E + 11	5.0E + 11	5.1E + 11	5.2E + 11	5.4E + 11	5.8E + 11
k_7	1.3E + 6	3.3E + 6	6.2E + 6	1.2E + 7	2.1E + 7	5.2E + 7	1.9E + 8
k_{-7}	2.6E + 4	6.4E + 4	7.8E + 4	2.2E + 5	3.5E + 5	8.0E + 5	2.5E + 6
k_9	2.8E + 5	7.1E + 5	1.0E + 6	2.7E + 6	4.5E + 6	1.1E + 7	4.0E + 7
k_{-9}	3.1E + 3	7.6E + 3	1.4E + 4	2.7E + 4	4.4E + 4	1.0E + 5	3.3E + 5

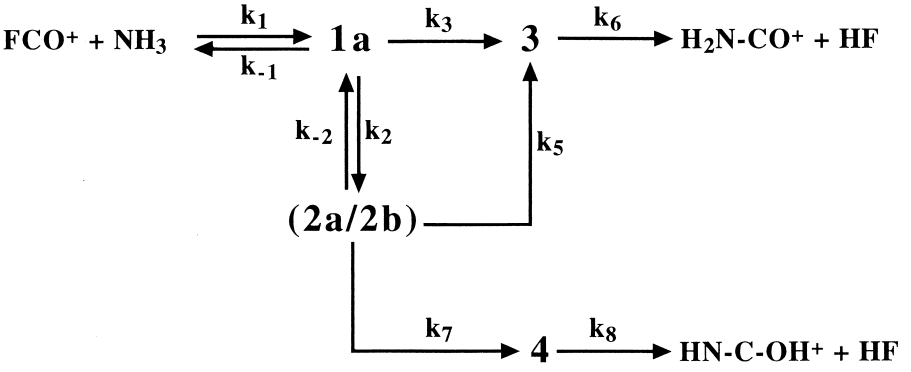

Chart 2.

occurs by any of the alternative mechanistic patterns derived from the kinetic scheme of Chart 2, it is possible to use the kinetic constants reported in Table 4 to calculate the corresponding value of **Eff(1)** for different internal energies **E** of the intermediate **1a**. The obtained values can be compared with the experimentally measured efficiency, 0.6 ± 0.2, used as a probing reference value.

If one denotes the full sequence of reactions reported in Chart 2 as *Mechanism 1*, the steady-state expression of the overall efficiency of reaction (1), **Eff(1, 1)**, is obtained as follows:

$$\textbf{Eff(1, 1)} = \frac{[k_3(k_{-2} + k_5 + k_7) + k_2k_5 + k_2k_7]}{[(k_{-2} + k_5 + k_7)(k_{-1} + k_2 + k_3) - k_2k_{-2}]}$$

and the values of **Eff(1, 1)** calculated as a function of **E** are reported in Table 5. This mechanistic proposal corresponds to the assumption that all of the three independent reaction patterns depicted in Chart 2 are simultaneously occurring. It is however possible to note that the contribution of the reaction path which involves the high-energy transition structure **TSOF2** is indeed negligible. In fact, if k_7 is set to zero, the values of **Eff(1, 1)** result the same as those reported in Table 5. We have subsequently evaluated the efficiency of reaction (1) by assuming that it occurs by only one of the three independent sequences denoted in Chart 3 as *Mechanism 2, Mechanism 3, and Mechanism 4*. The corresponding steady-state expressions of the overall efficiency of reaction (1), **Eff(1, 2)**, **Eff(1, 3)**, and **Eff(1, 4)** are derived as follows:

$$\textbf{Eff(1, 2)} = k_3/(k_{-1} + k_3)$$

$$\textbf{Eff(1, 3)} = k_2k_5/[k_{-2} + k_5)(k_{-1} + k_2) - k_2k_{-2}]$$

$$\textbf{Eff(1, 4)} = k_2k_7/[(k_{-2} + k_7)(k_{-1} + k_2) - k_2k_{-2}]$$

and the values calculated as a function of **E** are reported in Table 5. We note here that the values of **Eff(1, 2)** and **Eff(1, 3)** calculated by including the conceivable contribution of the reaction path which involves the transition structure **TSOF2**, i.e. by assuming a nonzero value of k_7, are identical to those reported in Table 5.

Based on our detailed kinetic analysis, we can do the following considerations about the detailed mechanism of reaction (1). It appears quite clear that the

Table 5
Efficiencies of reaction (1) calculated as a function of the energy content **E** of the intermediate **1a**

E (kcal mol^{-1})	**Eff(1, 1)**	**Eff(1, 2)**	**Eff(1, 3)**	**Eff(1, 4)**
70.1	1.00	1.00	1.00	1.00
72.1	0.70	0.55	0.52	0.01
73.6	0.56	0.39	0.36	0.01
75.5	0.29	0.18	0.16	0.00_3
77.0	0.17	0.10	0.08	0.00_2
80.0	0.04	0.03	0.02	0.00_1
85.0	0.01	0.00_4	0.00_2	

Mechanism 2

$$FCO^+ + NH_3 \underset{k_{-1}}{\overset{k_1}{\rightleftharpoons}} \mathbf{1a} \xrightarrow{k_3} \mathbf{3} \xrightarrow{k_6} H_2N\text{-}CO^+ + HF$$

Mechanism 3

$$FCO^+ + NH_3 \underset{k_{-1}}{\overset{k_1}{\rightleftharpoons}} (\mathbf{2a/2b}) \xrightarrow{k_5} \mathbf{3} \xrightarrow{k_6} H_2N\text{-}CO^+ + HF$$

Mechanism 4

$$FCO^+ + NH_3 \underset{k_{-1}}{\overset{k_1}{\rightleftharpoons}} (\mathbf{2a/2b}) \xrightarrow{k_7} \mathbf{4} \xrightarrow{k_8} HN\text{-}C\text{-}OH^+ + HF$$

Chart 3.

reaction path which involves the high-energy transition structure **TSOF2** has a negligible role. In fact, irrespective of the assumed value of **E**, the values of **Eff(1, 1)**, **Eff(1, 2)**, and **Eff(1, 3)** do not depend on k_7, and the values of **Eff(1, 4)** are exceedingly smaller than the experimental value of 0.6 ± 0.2. Therefore, the first important conclusion we draw is that the only expected ionic product from reaction (1) is the H_2N–CO^+ isomer. In addition, we note from Table 5 that, irrespective of the assumed internal energy content of **1a**, the value of **Eff(1, 1)** is invariably larger than **Eff(1, 2)** and **Eff(1, 3)**. Therefore, the second important conclusion we draw from our kinetic analysis is that *the most plausible mechanism of reaction (1) involves the simultaneous occurrence of two distinct reaction paths*. The first one is the "direct" HF elimination from the initially formed intermediate **1a** with formation of the ion-dipole adduct **3**, which eventually dissociates into the H_2N–CO^+ and HF constituent fragments. The second one requires prior isomerization of **1a** into the rapidly interconverting carbonium ions **2a** and **2b**, which in turn isomerize to the ion-dipole adduct **3**. Both of these reaction sequencies are essentially driven by the fact that the intermediate **1a** initially formed from the addition of FCO^+ to NH_3 has indeed energy enough to overcome the transition structures **TSNF**, **TSNO**, and **TSOF1**. In our FTICR experimental conditions, the differences of few kilocalories per mole computed between these three structures are not large enough to determine the selective occurrence of *Mechanism 2* or *Mechanism 3*. From Table 5, we note that the experimentally measured efficiency of reaction (1) practically matches the value calculated assuming the occurrence of the most plausible *Mechanism 1* at an energy content **E** of 73.6 kcal mol^{-1}, i.e. the energy content of **1a** generated from thermal FCO^+ and NH_3 at 298.15 K. It could be tempting to take this coincidence as a strong reinforcing evidence for *Mechanism 1*. However, it should not be overemphasized. In fact, all the *absolute* values of **Eff(1, i)** suffer of the fact that the kinetic constants k_{-1} have been computed at the MP2(FULL)/6-31$G(d)$ level of theory and are in principle less accurate than all the others $k_i s$, calculated at the $G2$ level of theory.

Acknowledgements

This work was financially supported by the Italian Ministero dell' Università e della Ricerca Scientifica e

Tecnologica (MURST) and the Consiglio Nazionale delle Ricerche (CNR).

References

[1] T.S. Sorensen, Angew. Chem. 110 (1998) 623; Angew. Chem. Int. Ed. Engl. 37 (1998) 603.
[2] W. Bleicher, P. Botschwina, Mol. Phys. 30 (1975) 1029.
[3] T.S. Zyubina, Zh. Neorg. Khim. 34 (1989) 1338.
[4] P. Pyykkö, Y. Zhao, J. Phys. Chem. 94 (1990) 7753.
[5] E.M. Sung, H.S. Lee, Bull. Korean Chem. Soc. 11 (1990) 511.
[6] P. Botschwina, P. Sebald, M. Bogey, C. Demuynck, J-L. Destombes, J. Mol. Spectrosc. 153 (1992) 255.
[7] Th. Krossner, M. Peric, R. Vetter, L. Zülicke, J. Chem. Phys. 101 (1994) 3981.
[8] J.S. Francisco, Chem. Phys. Lett. 265 (1997) 521.
[9] J. Hrušák, H. Schwarz, J. Phys. Chem. 97 (1993) 4659.
[10] G.K.S. Prakash, J.W. Bausch, G.A. Olah, J. Am. Chem. Soc. 113 (1991) 3203.
[11] G.A. Olah, A. Burrichter, T. Mathew, Y.D. Vankar, G. Rasul, G.K.S. Prakash, Angew. Chem. 109 (1997) 1958; Angew. Chem. Int. Ed. Engl. 36 (1997) 1875.
[12] (a) Z. Karpas, F.S. Klein, Int. J. Mass Spectrom. Ion Phys. 24 (1977) 137; (b) Z. Karpas, F.S. Klein, Int. J. Mass Spectrom. Ion Phys. 22 (1976) 189, and references therein.
[13] K.M. Johnson, I. Powis, C.J. Danby, Int. J. Mass Spectrom. Ion Phys. 32 (1979) 1.
[14] F. Grandinetti, F. Pepi, A. Ricci, Chem. Eur. J. 2 (1996) 495.
[15] L.A. Curtiss, K. Raghavachari, G.W. Trucks, J.A. Pople, J. Chem. Phys. 94 (1991) 7221.
[16] P.J. Robinson, K.A. Holbrook, Unimolecular Reactions, Wiley, New York, 1971.
[17] M.J. Frish, G.W. Trucks, H.B. Schlegel, P.M.W. Gill, B.G. Johnson, M.A. Robb, J.R. Cheeseman, T.A. Keith, G.A. Petersson, J.A. Montgomery, K. Raghavachari, M.A. Al-Laham, V.G. Zakrzewski, J.V. Ortiz, J.B. Foresman, J. Cioslowski, B.B. Stefanov, A. Nanayakkara, M. Challacombe, C.Y. Peng, P.Y. Ayala, W. Chen, M.W. Wong, J.L. Andres, E.S. Replogle, R. Gomperts, R.L. Martin, D.J. Fox, J.S. Binkley, D.J. Defrees, J. Baker, J.P. Stewart, M. Head-Gordon, C. Gonzalez, J.A. Pople, GAUSSIAN 94, Revision E.2 (Gaussian, Pittsburgh, PA, 1995).
[18] M.W. Schmidt, K.K. Baldridge, J.A. Boatz, S.T. Elbert, M.S. Gordon, J.H. Jensen, S. Koseki, N. Matsunaga, K.A. Nguyen, S.J. Su, T.L. Windus, M. Dupuis, J.A. Montgomery, J. Comput. Chem. 14 (1993) 1347.
[19] Selected reviews: (a) L.A. Curtiss, K. Raghavachari, in Quantum Mechanical Electronic Structure Calculations with Chemical Accuracy, S.R. Langhoff (Ed.), Kluwer Academic, Dordrecht, 1995; (b) K. Raghavachari, L.A. Curtiss, in Modern Electronic Structure Theory, D.R. Yarkony (Ed.), World Scientific, Singapore, 1995; (c) L.A. Curtiss, K. Raghavachari, in Computational Thermochemistry, K. Irikura, D.J. Frurip (Eds.), American Chemical Society Symposium Series 677 (1998).
[20] D.A. McQuarrie, Statistical Mechanics, Harper & Row, New York, 1976.
[21] (a) T. Beyer, D.R. Swinehart, ACM Commun. 16 (1973) 379; (b) R.G. Gilbert, S.C. Smith, Theory of Unimolecular and Recombination Reactions, Blackwell Scientific, Oxford, 1990.
[22] T. Baer, W.L. Hase, Unimolecular Reaction Dynamics, Oxford University Press, 1996.
[23] (a) S. Kato, K.J. Morokuma, J. Chem. Phys. 73 (1980) 3900; (b) W.H. Miller, N.C. Handy, J.E. Adams, ibid. 72 (1980) 99.
[24] FT-ICR/MS: Analytical Applications of Fourier Transform Ion Cyclotron Resonance Mass Spectrometry, B. Asamoto (Ed.), VCH, Weinheim, 1991.
[25] T. Su, M.T. Bowers, Int. J. Mass Spectrom. Ion Phys. 12 (1973) 347.
[26] Unless stated otherwise, all the experimental thermochemical data are taken from: S.G. Lias, J.A. Bartmess, J.F. Liebman, J.L. Holmes, R.D. Levin, W.G. Mallard, J. Phys. Chem. Ref. Data 17 (1988) Suppl. 1.
[27] T.J. Buckley, R.D. Johnson III, R.E. Huie, Z. Zhang, S.C. Kuo, R.B. Klemm, J. Phys. Chem. 99 (1995) 4879.
[28] C.E.C.A. Hop, J.L. Holmes, P.J.A. Ruttink, G. Schaftenaar, J.K. Terlow, Chem. Phys. Lett. 156 (1989) 251.
[29] W.H. Miller, Chem. Rev. 87 (1987) 19.